Observations of Laser-Beam Bending due to Transverse Plasma Flow

P. E. Young, C. H. Still, D. E. Hinkel, W. L. Kruer, E. A. Williams, R. L. Berger, and K. G. Estabrook

University of California, Lawrence Livermore National Laboratory, P.O. Box 808, Livermore, California 94550

(Received 3 February 1998)

Interferometric measurements of laser-produced channels in preformed plasmas show that in the presence of transverse plasma flow, the beam is deflected when the transverse flow velocity is near the sound speed. For a line focus with peak intensity of 1.5×10^{15} W/cm^2, a beam deflection of 10° is observed, which agrees well with the results of a three-dimensional hydrodynamics code. [S0031-9007(98)06886-0]

PACS numbers: 52.40.Nk, 52.35.Fp, 52.35.Mw, 52.50.Jm

The propagation of intense laser pulses through fully ionized plasmas can be affected by a number of processes which can be linear, such as refraction due to transverse density gradients, or nonlinear in the case of the filamentation instability. While laser-beam propagation in the direction normal to the density gradient and plasma flow have been studied thoroughly, transverse flow introduces new considerations and can, for example, influence the growth rate of filamentation [1]. This is of important consideration in hohlraum targets used in inertial confinement fusion applications where plasma flowing across the beam near the entrance hole can steer the beam. As a result, the symmetry of the intended x-ray drive can change because the position of the laser spot on the hohlraum wall is moved. Transverse flow steers the beam when the laser is sufficiently intense that the ponderomotive force causes the plasma to pile up against the upstream side of the beam which produces a density gradient that refracts the beam towards the downstream direction. This effect is particularly strong when the transverse flow velocity equals the sound speed of the plasma [1,2]. Although some evidence of this effect has recently been reported [3], quantitative comparison to theoretical predictions requires a well-characterized background plasma, and knowledge of the laser-beam path through the plasma.

In this Letter, we describe the results of an experiment in which we interferometrically observe the density channel produced by an intense laser-beam propagating through a preformed plasma. We observe beam bending in the presence of transverse plasma flow which increases as the laser intensity is increased, which rules out refractive effects due to the unperturbed density profile. An important point is that the beam bending occurs at a very low density ($\sim 0.05 n_c$) where the filamentation threshold is not exceeded. For a laser intensity of 1.5×10^{15} W/cm^2 we observe beam deflections of 10° which is in quantitative agreement with the predictions of the F3D hydrodynamic code [4]. The code uses the experimentally measured density and flow velocity profiles and a laser electric field reconstructed from the measured near-field phase profile of the experimental laser beam.

Some simple estimates illustrate the physics of beam bending. Consider a beam propagating through a flowing plasma with electron density n_e. A static equilibrium model between ponderomotive force, thermal pressure, and plasma flow predicts a density depression of magnitude $\delta n/n \sim (v_o/v_e)^2/(1 - M^2)$, where v_o is the electron quiver velocity in the laser field, v_e is the electron thermal velocity, and M is the Mach number of the flow component transverse to the direction of propagation. The density perturbation is swept downstream of the intensity maximum so that the light sees a refracting gradient $\nabla_\perp \delta n \sim (n_e/L_T)(v_o/v_e)^2(1 - M^2)^{-1}$, where L_T is the characteristic transverse dimension of the laser beam. By ray optics the light is deflected through an angle, θ, given by

$$\theta \sim \frac{1}{2n_c} \int \nabla_\perp \delta n \, dz = \frac{1}{2} \left(\frac{n_e}{n_c}\right) \left(\frac{v_o}{v_e}\right)^2 \frac{1}{L_T} \int \frac{dz}{1 - M(z)^2} . \qquad (1)$$

As $M \rightarrow 1$, the simple linear estimate for δn, above, fails. Within some range δM of the sonic point at $M = 1$, the density perturbation saturates, either nonlinearly ($\delta M \sim v_o/v_e$) [5] or from finite ion acoustic damping ($\delta M \sim \nu_{ia}/\omega_{ia}$, where ν_{ia}/ω_{ia} is the ion acoustic damping decrement) [6,7].

Independent of the saturation mechanism, and of the magnitude of δM ($\ll 1$), we can estimate the integral in Eq. (1) by $L_v/2$, where L_v is the scale length of the transverse velocity variation at the sonic point, giving

$$\theta \sim \frac{1}{4} \frac{n_e}{n_c} \left(\frac{v_o}{v_e}\right)^2 \frac{L_v}{L_T} . \qquad (2)$$

For a beam with internal structure, L_T can be expected to be characteristic of the typical hot spot dimensions, $\sim f\lambda$, rather than the total beam width. In this experiment, the beam phase was measured making quantitative comparison with numerical calculation well motivated.

Beam bending can occur whether or not the beam breaks up due to the filamentation instability. Existing hot spots

in the laser beam will be intensified by self-focusing, however. One anticipates from Eq. (2) that the increasing intensity and reduced lateral dimension of self-focused hot spots should increase beam bending. Strong filamentation, however, can be expected to cause beam breakup and the lack of identifiable channels.

An important point is that in this experiment, the observed beam bending occurs at a very low density before filamentation can occur, so filamentation is decoupled from the beam bending process. Filamentation results in the spraying of the beam and produces the termination of the channel near the peak of the plasma density, as observed by the interferometer. The imaginary wave number for ponderomotive filamentation is given by [8]

$$k_I = \frac{k_R}{2k_0}\left\{\frac{1}{2}\,\frac{\omega_0^2}{c^2}\,\frac{n_e}{n_c}\left(\frac{v_0}{v_e}\right)^2 - k_R^2\right\}^{1/2}, \qquad (3)$$

where k_R is the transverse size of the filaments. Since the beam width is only 20 μm, the filaments must be less than 10 μm in size to grow. For exponential growth, $2k_I L \simeq 1$. For the conditions $k_R/k_0 = 5$, $n/n_c = 0.05$, $T_{\mathrm{keV}} = 0.5$, $L_\mu = 50$, $\lambda_\mu = 1.064$, we find that $I_p = 4.5 \times 10^{15}$ W/cm^2 is required for exponential growth, which is 3 times the vacuum intensity. This analysis neglects the lowering of the background density in the beam channel, which would further raise the threshold intensity. In fact, both the experiments and the simulations show a well-defined channel all the way to the peak of the density profile ($\sim 0.3 n_c$) indicating that filamentation is not important at the lower densities.

The present experiment was conducted using the Janus laser at Lawrence Livermore National Laboratory where we have developed a test bed for studying the propagation of moderately intense laser pulses through well-characterized underdense plasmas [9]. A 1.064 μm wavelength, 100 ps full width at half maximum (FWHM) Gaussian pulse interacted with an underdense plasma formed by the irradiation of a 0.35 μm thick parylene [$(CH)_n$] foil by a 1 ns, 0.532 μm wavelength, 400 μm diameter, 2×10^{13} W/cm^2 laser pulse. Both a line focus and a circular focus were used for the interaction beam at various points in the experiment. A line focus (20 μm $\times$ 400 μm, peak intensity $= 1.5 \times 10^{15}$ W/cm^2) was used because the long path length through the channel makes the observed phase change due to the density depression easy to see [10]. To observe the behavior of the channel at higher intensities, we used a circular focus to achieve a peak intensity of 5×10^{16} W/cm^2. The best focus of the interaction beam in all cases is located at the target plane, and its measured vacuum properties [10] are constant as the laser intensity is varied by changing the amplifier gain which changes the laser energy. Varying the relative timing between the plasma formation and interaction pulses (1.5 to 2.5 ns delay from the end of the plasma forming pulse) determined the peak density ($0.25 n_c$ to $0.1 n_c$) seen by the interaction pulse. The background density profile was measured using a folded-wave interferometer. The 50 ps, 0.35 μm wavelength interferometer probe pulse arrived at the target at the same time as the peak of the 100 ps interaction pulse.

In order to introduce a component of the plasma flow that is transverse to the propagation direction of the interaction beam, the target foils are tilted at angles up to 45°. Since the plasma flow is normal to the target surface, the target angle determines the transverse flow velocity seen by the interaction pulse.

The main experimental results are summarized in Fig. 1. At the highest intensity (for a line focus), we see obvious

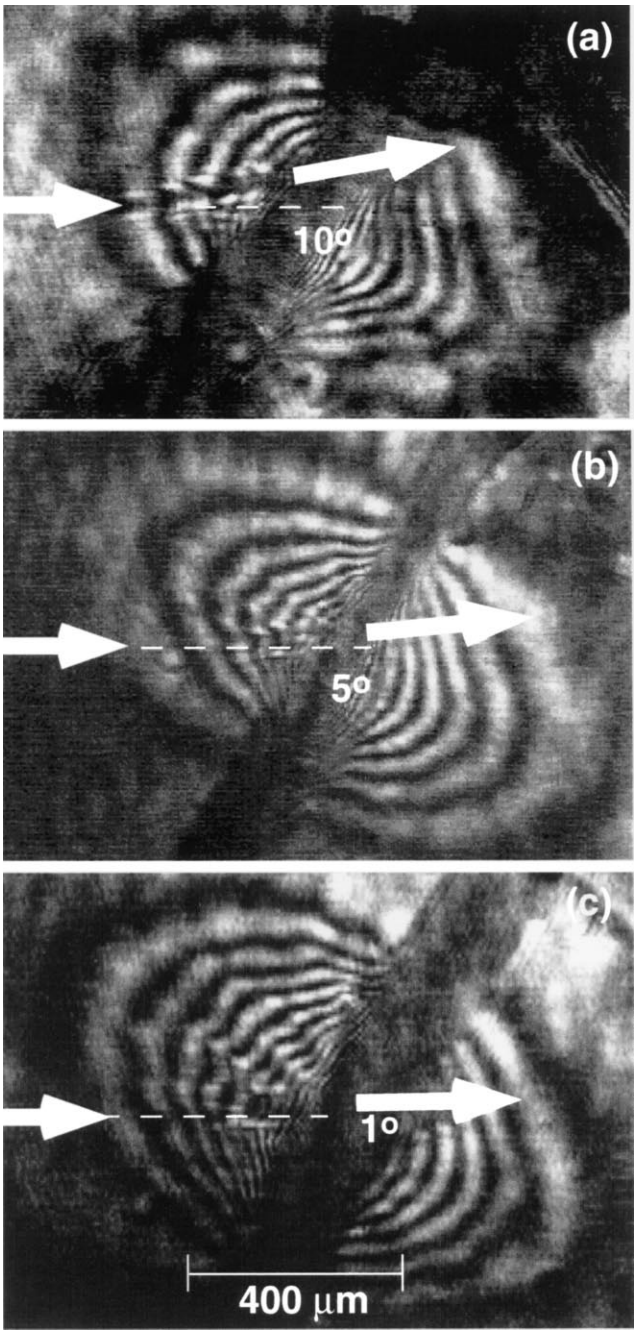

FIG. 1. Interferograms that show variation in channel bending for peak laser intensities of (a) 1.5×10^{15}, (b) 1×10^{15}, and (c) 5×10^{14} W/cm^2.

beam bending (~10°) at the outer edge of the plasma where the density is low (~$0.05n_c$) but the flow velocity is high (~1×10^8 cm/sec) compared to the sound speed, c_s (~3×10^7 cm/sec). The bending is localized and the channel stays well defined up to the peak plasma density (~$0.3n_c$) after which it disappears; this is because of beam breakup and spreading due to filamentation [10,11].

As we vary the incident laser intensity, the amount of bending becomes substantially less (see Fig. 1) until there is a 1° deflection for an intensity of 2×10^{14} W/cm^2, clearly showing that this is an intensity dependent effect and not due to linear refraction in the inhomogeneous plasma distribution. We observe a similar reduction in bending angle as we decrease the target angle, as expected.

The deflection predicted by the simple analytic model of Eq. (2) agrees well with that observed in the experiment. For the line focus, we take $n/n_c \simeq 0.05$, $I = 1 \times 10^{15}$ W/cm^2, $T_e = 500$ eV, $L_v \simeq 200$ μm, and $L_T \simeq 10$ μm, and find $\theta \simeq 13°$, close to what is observed in the experiment. Of course, quantitative calculations need to account for detailed beam structure, laser-beam filamentation, and various three-dimensional effects. For example, when a circular focus is used to obtain a very high intensity (5×10^{16} W/cm^2), no beam deflection is detected. This result is in agreement with the nonlinear model of Rose [6,12], who has discussed a regime in which the plasma can simply flow around a small beam, an effect which clearly decreases the deflection.

We identify the location of the beam bending that occurs where the flow velocity equals the inferred sound speed, c_s, by obtaining plasma interferograms at different times (100 ps steps) relative to the end of the plasma forming pulse on sequential irradiations of the target. We then Abel invert the interferograms to obtain the plasma density distribution. By using the continuity equation $\partial n_e/\partial t = \nabla \cdot (n_e \mathbf{v})$, where $\mathbf{v}$ is the flow velocity, we can recover the velocity distribution of the plasma, using the boundary condition $v = 0$ at the peak of the density profile. We also assume that $\mathbf{v}$ is parallel to ∇n_e. The results are shown in Fig. 2 for the conditions of Fig. 1; we find a transverse flow velocity of 2×10^7 cm/s which is close to both the sound speed inferred from earlier Thomson scattering measurements ($T_e = 700$ eV) on solid carbon targets [13] and the prediction of two-dimensional LASNEX simulations ($T_e = 300$ eV).

The experimental results are compared to numerical simulations in order to understand the laser propagation behavior. We used a version of the F3D code [4] that incorporated a fully 3D nonlinear Eulerian hydrodynamics package (NH3) in Cartesian coordinates. F3D is a fully nonlinear, time dependent code in which the hydrodynamic and heat transport are coupled to the light wave propagation.

The experiment was duplicated in the simulation as much as possible. We modeled the electric field and phase distributions of the interaction beam by using an input phase profile that was experimentally measured using radial shear interferometry and numerically propagating the beam through the lenses used in the experiment (aspheric lens, 20 cm focal length, and two −3.94 m focal length cylindrical lenses which were crossed at a 45° angle to produce the appropriate line focus length). The calculated intensity distribution agrees well with equivalent plane images that were obtained from the experiment (see Fig. 3). The 100 ps Gaussian pulse shape used in the experiment is modeled in the simulations by a smoothly rising ramp, $S(t) = 1 - [1 - (t/t_p)^2]^2$, where $t_p = 100$ ps. The measured electron density and flow velocity profiles [see Fig. 2(b)] were used as the initial conditions for the simulation. Because of the narrow cross section of the laser beam it is only necessary to model a region with transverse dimension of 120 μm and axial dimension of 350 μm. Over this transverse scale, the density and flow can be taken as uniform along the transverse direction initially but both vary along the axial laser propagation direction. Even after the beam deflects at low density and filaments at higher density, the beam stayed away from the simulation edges as shown in the example in Fig. 4. The electron temperature is initially uniform with values taken between 300 and 700 eV to bracket the LASNEX predictions and the Thomson scattering measurements; best agreement with the experiment is found for $T_e = 500$ eV.

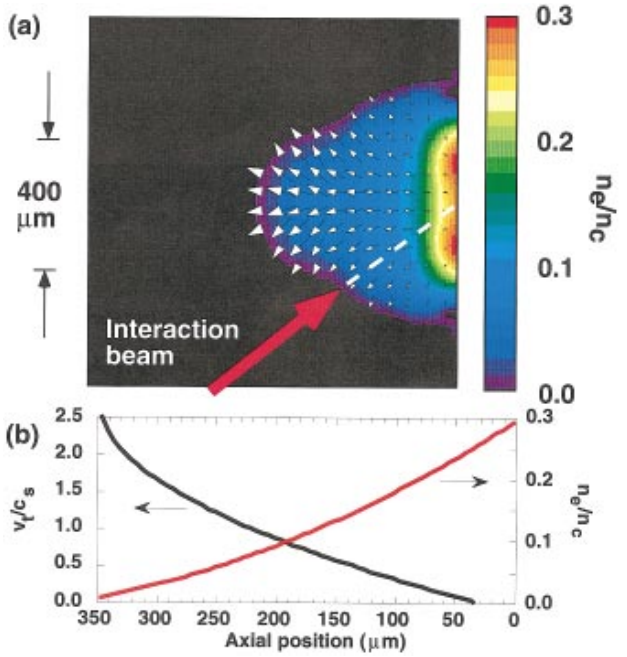

FIG. 2(color). Shown are (a) density and flow velocity distributions calculated from the experimental data (the longest arrow corresponds to a flow velocity of 1.4×10^8 cm/sec), and (b) density and transverse velocity (normalized to the sound speed) profiles along the axis of the interaction pulse.

Figure 4 shows the calculated density channels, averaged over 50 ps centered on the peak of the laser pulse, that are formed in the background density profile. Figure 4(a) shows the laser-beam path when the plasma flow

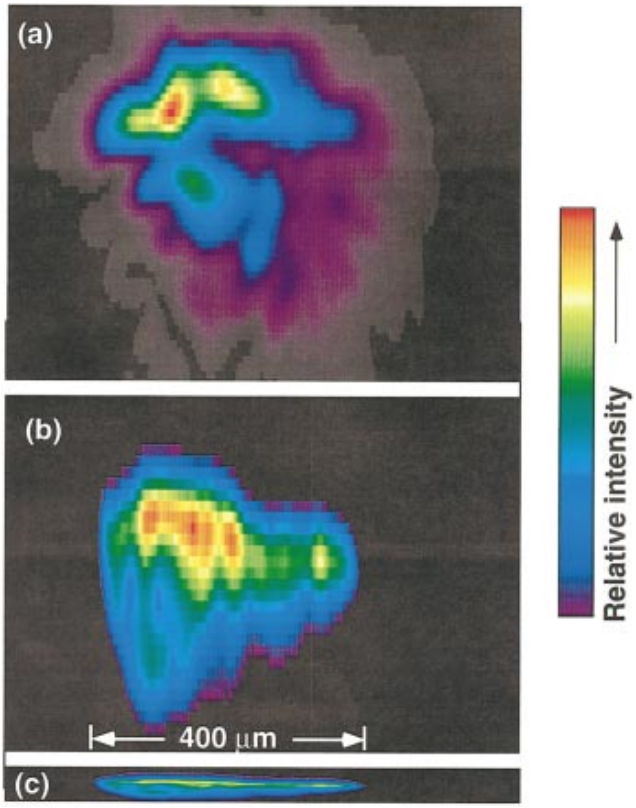

FIG. 3(color). Comparison of (a) the calculated intensity using the measured near-field phase front profile, and (b) the equivalent target plane image of the line focus. The vertical scales of (a) and (b) have been expanded (box heights are 40 μm versus 500 μm for the width of the boxes) to facilitate comparison of the detailed intensity structure. The measured spot in normal aspect ratio is shown in (c).

(both axial and transverse) is turned off in the simulation. The channel follows the asymmetry of the beam spot seen in Fig. 3 as it propagates through the beam waist; this is more apparent here than in the experiment due to the spatial scale of the figure and the presence of fine scale structure which is not resolved in the line-averaged interferometer measurement. When the experimental flow profile is introduced, the simulation [see Fig. 4(b)] clearly shows a bend of about 10°, in agreement with the experiment. The initial bend is at the sonic point for an initial temperature of 500 eV. The channel persists without filamenting for 200 μm past the sonic point in good agreement with the experiment. A fraction of the energy continues to show up in the undeviated channel, which is also seen in the original interferograms.

In conclusion, we have quantitatively measured the beam deflection in a plasma due to transverse plasma flow. The deflection at moderate intensities is predicted

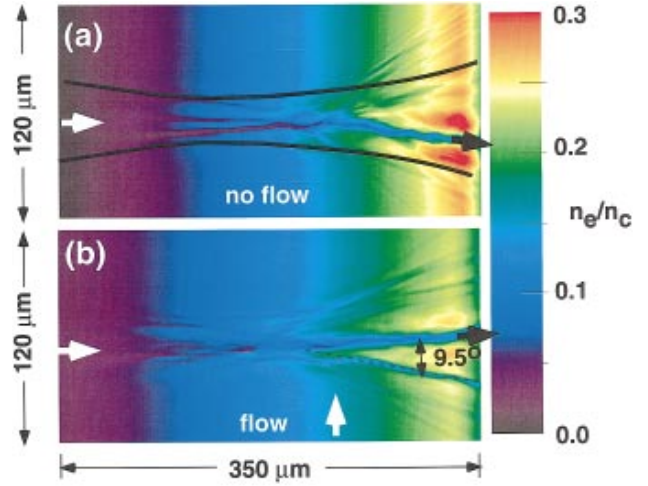

FIG. 4(color). Density distributions calculated by F3D using the experimental density profile (a) with no plasma flow, and (b) with the experiment flow velocity profile. The simulation has been averaged over 50 ps centered on the peak of the pulse. The laser enters from the left side of the box and propagates to the right. The solid lines in (a) show the location of the $1/e$ intensity contour of the beam profile.

well by a simple analytic model. A nonlinear hydrodynamic model using the experimental laser-beam electric field profile, plasma density, and flow velocity distributions shows excellent agreement with the experiment.

We thank W. Seka for valuable discussions concerning the near-field phase front measurement of the laser beam. We thank J. Hunter, G. London, B. Sellick, and J. Foy for technical assistance during the experiment. This work was performed under the auspices of the U.S. Department of Energy by the Lawrence Livermore National Laboratory under Contract No. W-7405-Eng-48.

[1] R. W. Short *et al.*, Phys. Fluids **25**, 2302 (1982).
[2] D. E. Hinkel *et al.*, Phys. Rev. Lett. **77**, 1298 (1996).
[3] J. D. Moody *et al.*, Phys. Rev. Lett. **77**, 1294 (1996).
[4] R. L. Berger *et al.*, Phys. Fluids B **5**, 2243 (1993).
[5] W. L. Kruer and J. H. Hammer, Comments Plasma Phys. Control. Fusion **18**, 85 (1997).
[6] H. A. Rose, Phys. Plasmas **3**, 1709 (1996).
[7] D. E. Hinkel *et al.*, Phys. Plasmas **5**, 1887 (1998).
[8] W. L. Kruer, Comments Plasma Phys. Control. Fusion **9**, 63 (1985).
[9] P. E. Young *et al.*, Phys. Rev. Lett. **75**, 1082 (1995).
[10] P. E. Young *et al.*, Phys. Plasmas **2**, 2825 (1995).
[11] S. C. Wilks *et al.*, Phys. Rev. Lett. **73**, 2994 (1994).
[12] S. Ghosal and H. A. Rose, Phys. Plasmas **4**, 2376 (1997).
[13] P. E. Young, Phys. Rev. Lett. **73**, 1939 (1994).